Journal of Engineering and Applied Sciences 12 (Special Issue 10): 8919-8923, 2017
ISSN: 1816-949X

Hydrophobic Sol-Gel Anti-Reflective Coating with Various Sized Silica Nanoparticles

Ki-Chul Kim
Department of Advanced Chemical Engineering, Mokwon University,
88 Doanbook-ro, Seo-gu, 35349 Daejeon, Korea

Abstract: Functional coatings, Anti-Reflection (AR), self-cleaning and anti-fogging have been applied to cover glass of crystalline silicon photovoltaic cells to increase the efficiency of photo-electric conversion. In this study, hydrophobic AR coatings with various sized silica Nanoparticles (NPs) were fabricated on slide glass substrate by sol-gel process and spin-coating process. The surface shape of the AR coating films was investigated by a field emission scanning electron microscope and scanning probe microscope. The measurement of contact angle was performed to confirm the hydrophobicity. The transmittance of the AR coating layers was estimated by an UV-visible spectrometer. The results showed that the AR coating layers of 30, 100 and 150 nm silica NPs exhibit hydrophobic characteristic with contact angle of over 115°. The average transmittance of 7 nm silica NPs coating thin layer exhibits 3.3% higher than one of the bare slide glass substrate per single side coating in the visible light range. The most effective AR coating layer is 7 nm silica NPs coating while AR coating layer of 100 nm silica NPs coating exhibits most hydrophobic characteristic of 123.4°. The optimum functional coating, anti-reflective and hydrophobic coating surface was 30 nm silica NPs coating layer with the average transmittance of 91.2% and contact angle of 116°. The hydrophobic AR coating with 30 nm silica nanoparticles is capable of application for cover glass of photovoltaic cells.

Key words: Hydrophobic, sol-gel process, anti-reflection, silica nanoparticles, functional coating, average

INTRODUCTION

Crystalline silicon solar cells need a protection layer, which preserves the photovoltaic cells from external shocks and corrosion (Han *et al*., 2009). But this protection layer induces the reflection of sunlight. The reflection of sunlight leads to reduce the efficiency of photo-electric conversion. The cover glass of photovoltaic cells which has refractive index of 1.52, reflects around 4% of normally incident light on each air/substrate interface (Chhajed *et al*., 2008). The Anti-Reflection (AR) coating is usually applied to the protection layer to reduce sunlight reflection and to increase sunlight transmittance (Han *et al*., 2009; Chhajed *et al*., 2008). The AR coated cover glass can improve photovoltaic cell's efficiency. For outdoor applications, not only high transmittance but also self-cleaning function is desirable (Faustini *et al*., 2010; Kesmez *et al*., 2009; Nakajima *et al*., 2000). The hydrophobic surface leads to self-cleaning function. The high contact angle, hydrophobic surface, causes to form spherical-like droplets which simply roll off carrying away contaminant and dust (Nakajima *et al*., 2000).

To complete perfect anti-reflection, the various technologies have been extensively investigated such as multi-layer vacuum deposition (Kim, 2015, 2016), sol-gel dip or spin coating (Liu and Yeh, 2010), bio-mimic moth-eye anti-reflection structures (Li *et al*., 2010; Yamada *et al*., 2011) and self-assembled colloidal dip coating (Askar *et al*., 2013). Among many available AR coating technologies, sol-gel AR coating using the silica Nanoparticles (NPs) is a promising approach. Because it is inexpensive, fast and simple method (Askar *et al*., 2013). In this study, various sized silica NPs were synthesized by sol-gel process with Tetra Ethyl Ortho Silicate (TEOS) (Gao and He, 2013). AR coatings were fabricated by spin-coating process using the silica NPs sols on the cleaned slide glass. The hydrophobic surfaces were prepared by spin-coating process with the diluted solution of methyl alcohol and 1H, 1H, 2H, 2H-Perfluorodecyltrimethoxysilane on silica NPs coating/slide glass. The surface shape of the AR coating layers was investigated by a FE-SEM (Field Emission Scanning Electron Microscope) and SPM (Scanning Probe Microscope). The hydrophobic characteristic was investigated by a contact angle measurement. The optical properties of the AR coating layers with various sized silica NPs were investigated by an UV-visible spectrometer.

MATERIALS AND METHODS

Synthesis of SiO_2 nanoparticles and fabrication of hydrophobic anti-reflective coating: The various sized silica NPs sols were synthesized by the hydrolysis process and condensation process of TEOS (Samchun, 95%) in ethyl alcohol (Samchun, 94.5%) and in presence of ammonium hydroxide solution (Sigma-Aldrich, 28%) as catalyst. The size of silica NPs was adjusted by the TEOS and ammonium concentration. The substrates of slide glass were subsequently cleaned with acetone, ethanol and DI water in ultrasonic bath. The cleaned slide glass was dried by air gun with high purity nitrogen gas of 99.999%. The AR coating films were fabricated on cleaned slide glass by spin-coating process with 3.000~6.000 rpm. The hydrophobic surfaces were functionalized by spin-coating process using the diluted solution of methyl alcohol and 1H, 1H, 2H, 2H-Perfluorodecyltrimethoxysilane on silica NPs coating layers.

Characterization of hydrophobic AR coating layer: The surface morphology of AR coating layers on slide glass was characterized by a FE-SEM (FEI, Sirion) and SPM (Park System, XE-100). The hydrophobic surface exhibits concavo-convex structures with a nanoscale (Wang and Shu, 2013; Purcar *et al*., 2012; Glaubitt and Lobmann, 2011; Howarter and Youngblood, 2008). To investigate the surface structure of anti-reflective coating layers, the surface roughness of the anti-reflective coating films was characterized by an SPM with non-contact mode. But excessive concavo-convex structure of AR coating surface induces the diffused reflection which causes the low transmittance. The hydrophobic characteristic of the AR coating films was analyzed by a contact angle measurement (SEO Co. Ltd., Phoenix 300 Plus). The transmittance of the AR coating films on slide glass was measured by an UV-visible spectrometer in the range of 300~1.100 nm wavelength.

RESULTS AND DISCUSSION

The various sized SiO_2 nanoparticles were synthesized by the stöber sol-gel process. The particle size of silica NPs was controlled by adjusting of concentration of TEOS and ammonium hydroxide solution. The particle size and morphology of the various sized silica NPs were investigated by a FE-SEM which was shown in Fig. 1. The silica NPs exhibit spherical shape and there is no wide distribution in the particle

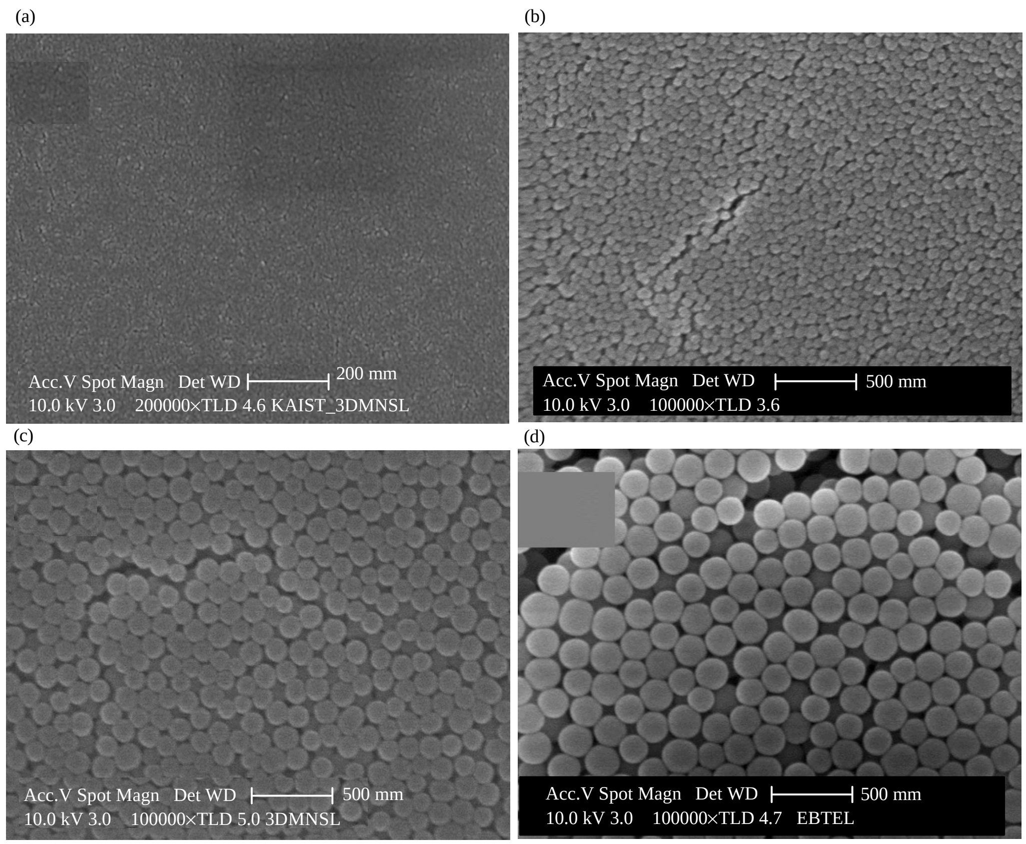

Fig. 1: FE-SEM images of the: a) 7 nm SiO_2 NPs (Nanoparticles) thin layer; b) 30 nm SiO_2 NPs thin layer; c) 100 nm SiO_2 NPs thin layer and d) 150 nm SiO_2 NPs thin layer which were coated by spin-coating process on cleaned slide glass

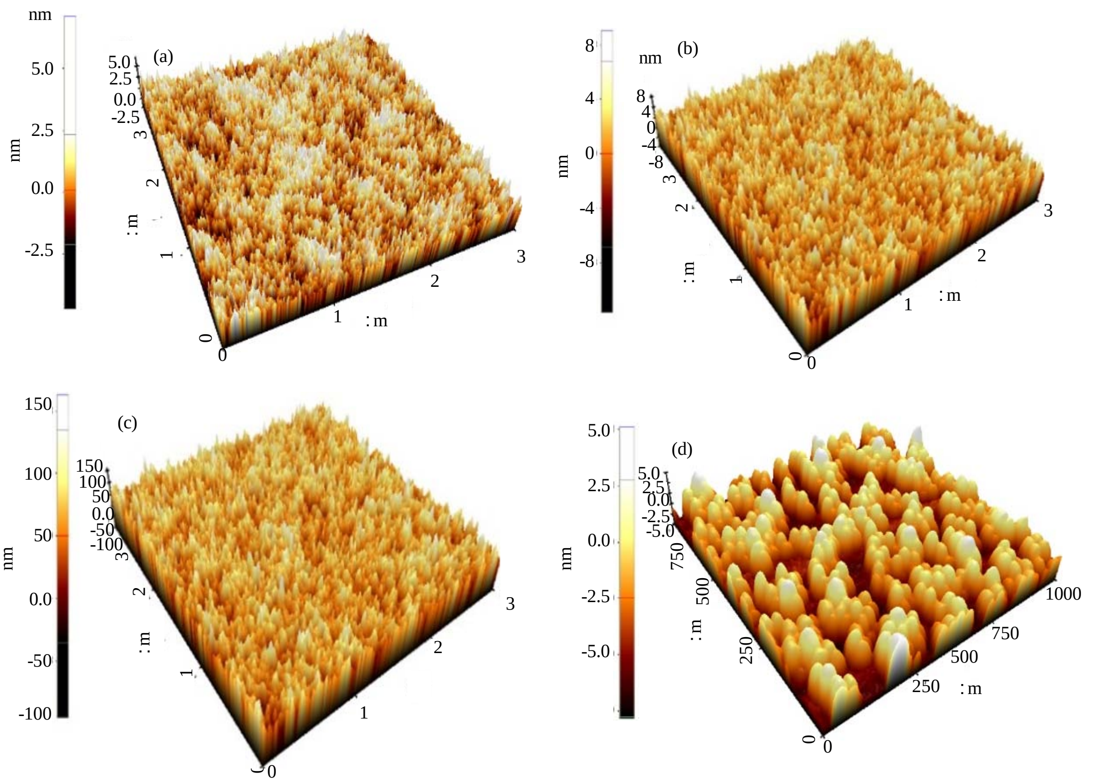

Fig. 2: SPM images of the: a) 7 nm SiO_2 NPs coating surface; b) 30 nm SiO_2 coating surface; c) 100 nm SiO_2 NPs coating surface and d) 150 nm SiO_2 coating surface by spin-coating process on cleaned slide glass which were analyzed with the non-contact mode

sizes but not monodispersed. The particle size of silica NPs increases with the TEOS and ammonium concentration (Ibrahim *et al*., 2010). The average particle size of the synthesized silica NPs was 7, 30, 100 and 150 nm, respectively. The surface morphology of the various sized silica NPs coating layers on slide glass by a spin-coating process was quite smooth.

The surface reflection of AR coating layer is affected by the surface roughness of anti-reflective coating layer. The surface roughness of the silica NPs coating layers were analyzed by SPM with non-contact mode. The SPM images of the various sized silica NPs coating surfaces were shown in Fig. 2. The surface of 7 nm silica NPs coating layer exhibits very smooth characteristic. The surface of 30 nm silica NPs coating layer and 150 nm silica NPs coating layers exhibit quite smooth characteristic but the surface of 100 nm silica NPs coating layer exhibits quite concavo-convex structure. The average surface roughness was measured around 0.89, 1.70, 40.38 and 1.44 nm for 7 nm SiO_2 nanoparticles coating layer, 30 nm SiO_2 nanoparticles coating layer, 100 nm SiO_2 nanoparticles coating layer and 150 nm SiO_2 nanoparticles coating layer, respectively.

The hydrophobic surface derives self-cleaning function (Nakajima *et al*., 2000; Gao and He, 2013; Wang and Shu, 2013). To confirm the hydrophobic characteristic, the contact angle measurements were carried out for various sized silica NPs coating layers. The images of contact angle measurement were shown in Fig. 3 for various sized silica NPs coating layers. The measured values of contact angle were 65.5°, 115.8°, 123.4° and 114.6° for 7 nm SiO_2 nanoparticles coating layer, 30 nm SiO_2 nanoparticles coating layer, 100 nm SiO_2 nanoparticles coating layer and 150 nm SiO_2 nanoparticles coating layer, respectively. The silica NPs coating layers of 30, 100 and 150 nm exhibit quite hydrophobic characteristic but silica NPs coating layer of 7 nm exhibits a little hydrophobic characteristic. The silica NPs coating layer of 100 nm exhibits most hydrophobic characteristic of 123.4° which is attributed to the concavo-convex surface structure and functional hydrophobic treatment. The high values of contact angle of 30, 100 and 150 nm silica nanoparticles coating layers are expected to operate the self-cleaning function.

The transmittance curves of the bare slide glass, silica NPs coating layers of 7, 30, 100 and 150 nm were measured

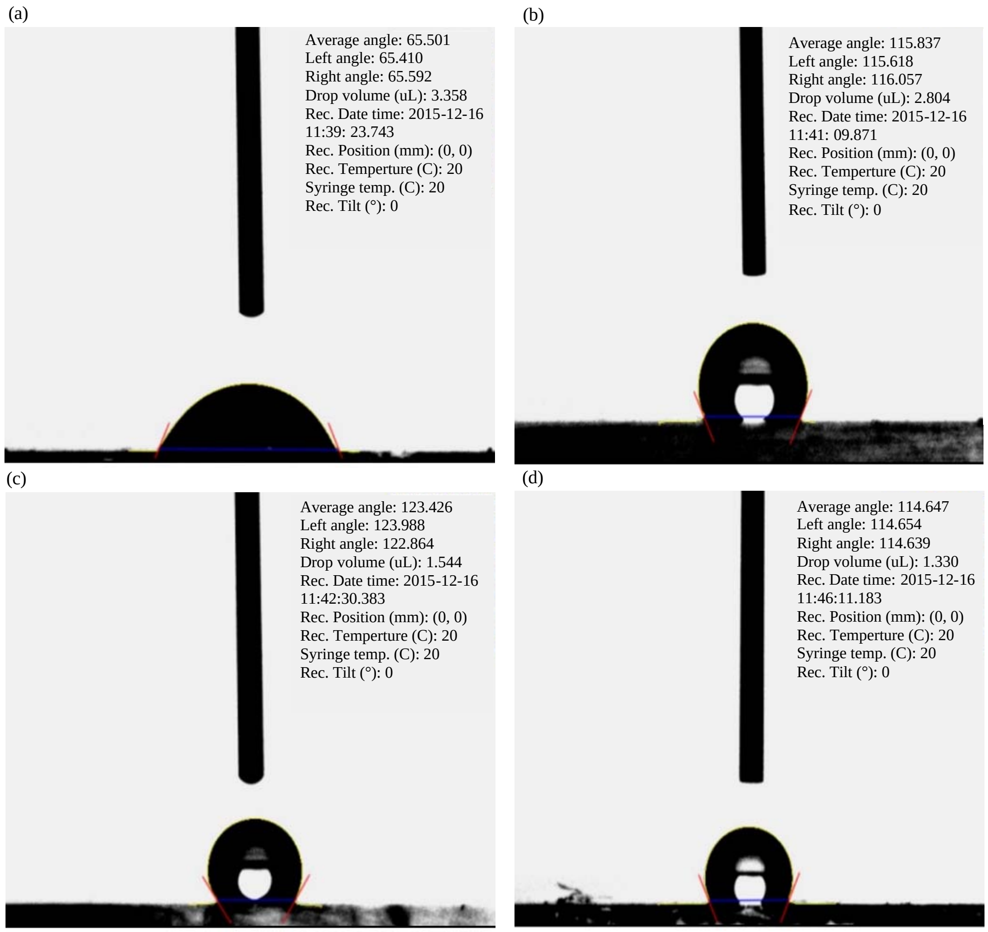

Fig. 3: Contact Angle (CA) measurement images of the: a) 7 nm SiO_2 NPs coating surface; b) 30 nm SiO_2 NPs coating surface; c) 100 nm SiO_2 NPs coating surface and d) 150 nm SiO_2 NPs coating surface which were coated by spin-coating process on cleaned slide glass. The measured CA values were 65.5°, 115.8°, 123.4° and 114.6°, respectively

by an UV-visible spectrometer in the range of 300~1.100 nm wavelength. The average transmittance of the bare slide glass was 90.0% in the visible light range (400~800 nm). As shown in Fig. 4, the mean transmittance of the silica NPs anti-reflective coating layers of 7, 30, 100 and 150 nm were 93.3, 91.2, 90.5 and 89.6% in the visible light range, respectively. The most effective AR coating layer was 7 nm silica NPs coating layer which was exhibited 3.3% higher than one of the bare slide glass substrate per single side coating. But hydrophobic characteristic of the 7 nm silica NPs coating layer is not excellent. The optimum functional coating, anti-reflective and hydrophobic coating surface was 30 nm silica NPs coating layer with the average transmittance of 91.2% and contact angle of 115.8°. It is attributed to the optimal porosity and surface roughness (Moghal *et al*., 2012; Kuo *et al*., 2008).

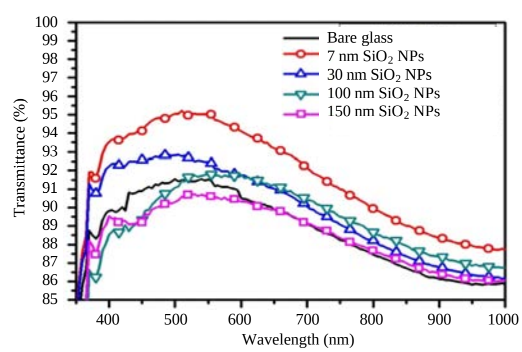

Fig. 4: Transmittance curves of the bare slide glass, 7 nm SiO_2 NPs coating layer, 30 nm SiO_2 NPs coating layer, 100 nm SiO_2 NPs coating layer and 150 nm SiO_2 NPs coating layer with a hydrophobic surface which were coated by spin-coating process on cleaned slide glass

CONCLUSION

The protective cover glass of crystalline silicon photovoltaic cells is required high transmittance and hydrophobic surface characteristic which is operated to self-cleaning function. The various sized SiO_2 nanoparticles were synthesized by the stöber sol-gel process. The particle size effect of silica nanoparticles for functional AR coating and hydrophobic surface characteristic have been demonstrated to be capable of increasing transmittance of protective cover glass. The AR characteristic and hydrophobic surface property is affected by surface roughness and porosity of coating layer. The optimal particle size of AR coating and hydrophobic surface characteristic was 30 nm silica nanoparticles.

ACKNOWLEDGEMENTS

This research (Grant No. C0397062) was supported by Business for Cooperative R&D between Industry, Academy and Research Institute funded Korea Small and Medium Business Administration in 2016.

REFERENCES

Askar, K., B.M. Phillips, Y. Fang, B. Choi and N. Gozubenli *et al*., 2013. Self-assembled self-cleaning broadband anti-reflection coatings. Colloids Surf. A. Physicochemical Eng. Aspects, 439: 84-100.

Chhajed, S., M.F. Schubert, J.K. Kim and E.F. Schubert, 2008. Nanostructured multilayer graded-index antireflection coating for SI solar cells with broadband and omnidirectional characteristics. Appl. Phys. Lett., 93: 251108-1-251108-3.

Faustini, M., L. Nicole, C. Boissiere, P. Innocenzi and C. Sanchez *et al*., 2010. Hydrophobic, antireflective, self-cleaning and antifogging sol gel coatings: An example of multifunctional nanostructured materials for photovoltaic cells. Chem. Mater., 22: 4406-4413.

Gao, L. and J. He, 2013. A facile dip-coating approach based on three silica sols to fabrication of broadband antireflective superhydrophobic coatings. J. Colloid Interface Sci., 400: 24-30.

Glaubitt, W. and P. Lobmann, 2011. Anti-soiling effect of porous SiO2 coatings prepared by sol-gel processing. J. Sol Gel Sci. Technol., 59: 239-244.

Han, K.S., H. Lee, D. Kim and H. Lee, 2009. Fabrication of anti-reflection structure on protective layer of solar cells by hot-embossing method. Solar Energy Mater. Solar Cells, 93: 1214-1217.

Howarter, J.A. and J.P. Youngblood, 2008. Self-cleaning and next generation anti-fog surfaces and coatings. Macromol. Rapid Commun., 29: 455-466.

Ibrahim, I.A., A.A.F. Zikry and M.A. Sharaf, 2010. Preparation of spherical silica nanoparticles: Stober silica. J. Am. Sci., 6: 985-989.

Kesmez, O., H.E. Camurlu, E. Burunkaya and E. Arpac, 2009. Sol-gel preparation and characterization of anti-reflective and self-cleaning SiO2-TiO2 double-layer nanometric films. Solar Energy Mater. Solar Cells, 93: 1833-1839.

Kim, K.C., 2015. Effective graded refractive-index anti-reflection coating for high refractive-index polymer ophthalmic lenses. Mater. Lett., 160: 158-161.

Kim, K.C., 2016. Anti-reflection coating technology based high refractive index lens with ultra-violet rays blocking function. J. Korea Acad. Ind. Cooperation Soc., 17: 482-487.

Kuo, M.L., D.J. Poxson, Y.S. Kim, F.W. Mont and J.K. Kim *et al*., 2008. Realization of a near-perfect antireflection coating for silicon solar energy utilization. Opt. Lett., 33: 2527-2529.

Li, Y., J. Zhang and B. Yang, 2010. Antireflective surfaces based on biomimetic nanopillared arrays. Nano Today, 5: 117-127.

Liu, B.T. and W.D. Yeh, 2010. Antireflective surface fabricated from colloidal silica nanoparticles. Colloids Surfaces A: Physicochem. Eng. Aspects, 356: 145-149.

Moghal, J., J. Kobler, J. Sauer, J. Best and M. Gardener *et al*., 2012. High-performance, single-layer antireflective optical coatings comprising mesoporous silica nanoparticles. ACS. Appl. Mater. Interfaces, 4: 854-859.

Nakajima, A., K. Hashimoto, T. Watanabe, K. Takai and G. Yamauchi *et al*., 2000. Transparent superhydrophobic thin films with self-cleaning properties. Langmuir, 16: 7044-7047.

Purcar, V., I. Stamatin, O. Cinteza, C. Petcu and V. Raditoiu *et al*., 2012. Fabrication of hydrophobic and antireflective coatings based on hybrid silica films by sol-gel process. Surf. Coat. Technol., 206: 4449-4454.

Wang, S.D. and Y.Y. Shu, 2013. Superhydrophobic antireflective coating with high transmittance. J. Coat. Technol. Res., 10: 527-535.

Yamada, N., O.N. Kim, T. Tokimitsu, Y. Nakai and H. Masuda, 2011. Optimization of anti-reflection moth-eye structures for use in crystalline silicon solar cells. Prog. Photovoltaics Res. Appl., 19: 134-140.